Design of Shaped-Beam Reflectarrays with Arbitrary Geometrical Constraints: An Inverse Source Approach

M. Salucci, A. Gelmini, G. Oliveri, N. Anselmi, and A. Massa

Abstract

In this work, an innovative paradigm is presented to deal with the design of reflectarray surface currents that satisfy both radiation and arbitrary geometry constraints. To this aim, the synthesis problem at hand is formulated as an inverse source one, then solved in an analytical way. Owing to the non-uniqueness of the solution, the existence of non-radiating current components are successfully exploited as additional degrees-of-freedom to match both radiation and aperture geometry constraints. Selected representative numerical experiments are presented to verify the effectiveness of the developed synthesis method.

Contents

1 Numerical Results

1.1 Shape "triangle @ down left corner: 2 pixel side"

Parameters

- Number of reflectarray elements: $M = N = 55$;
- Operative frequency: $f = 14$ [GHz];
- Polarization: X-CO;
- Number of elements in the forbidden region: $Q = 3$;

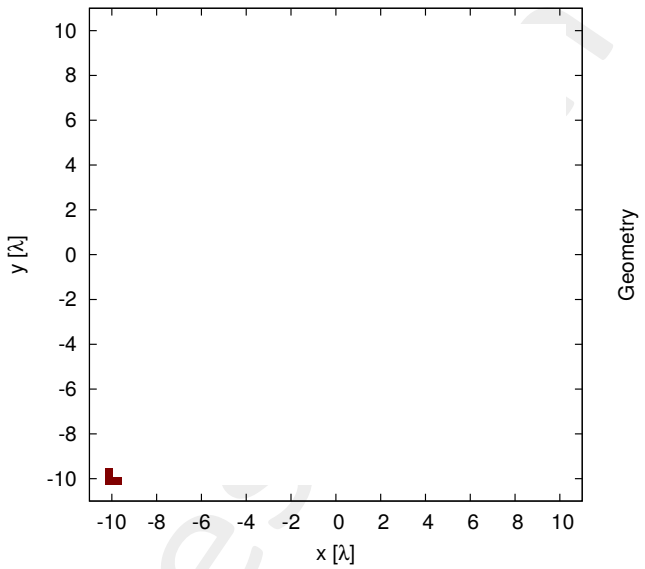

Figure 1: Geometry of forbidden region Ω.

Results

Magnitude and phase of the *NR* coefficients.

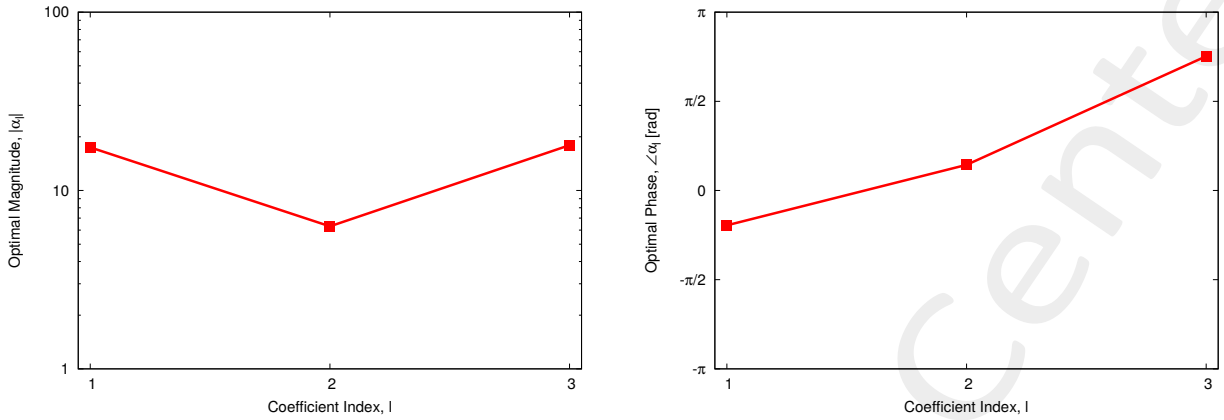

(*a*) (*b*)

Figure 2: Magnitude (*a*) and phase (*b*) of the solution.

Currents Distribution

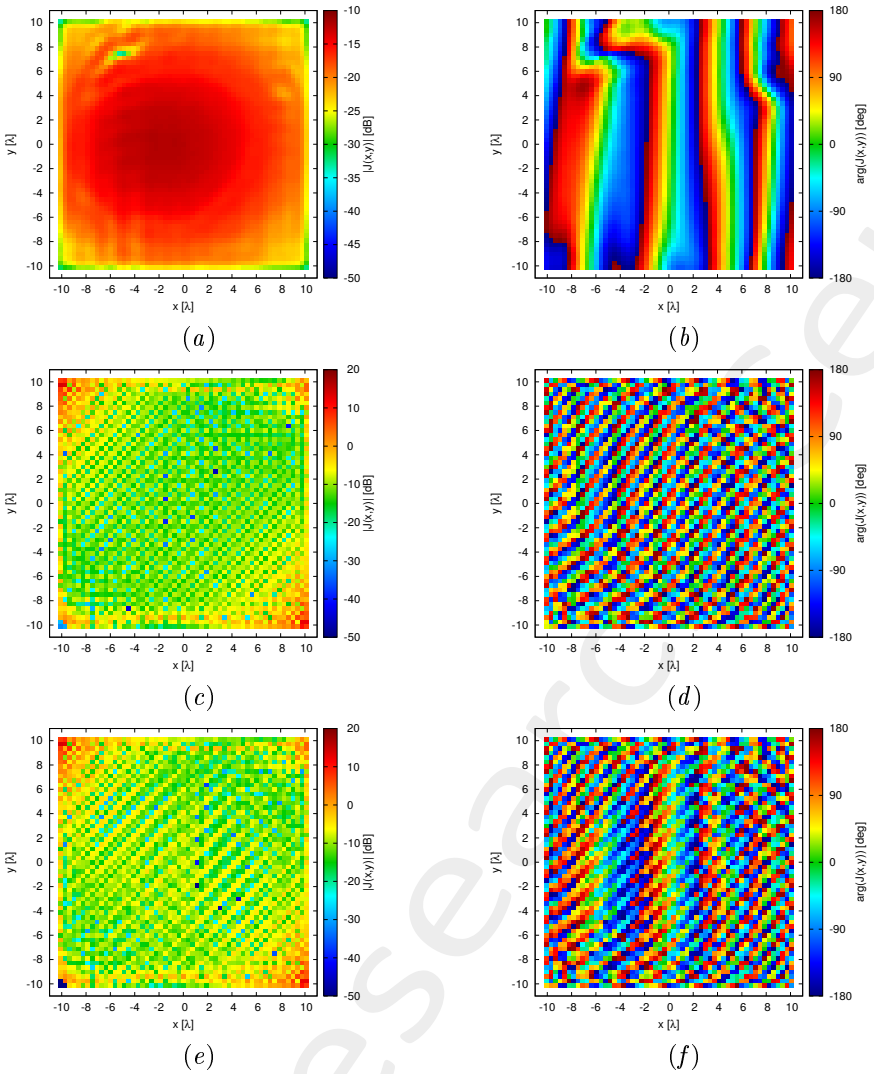

Figure 3: $(a)(c)(e)$ Magnitude and $(b)(d)(f)$ phase $(a)(b)$ of $J^{MN}(x,y)$, $(c)(d)$ $J^{NR}(x,y;\underline{\alpha})$, and $(e)(f)$ $J^{TOT}(x,y;\underline{\alpha})$.

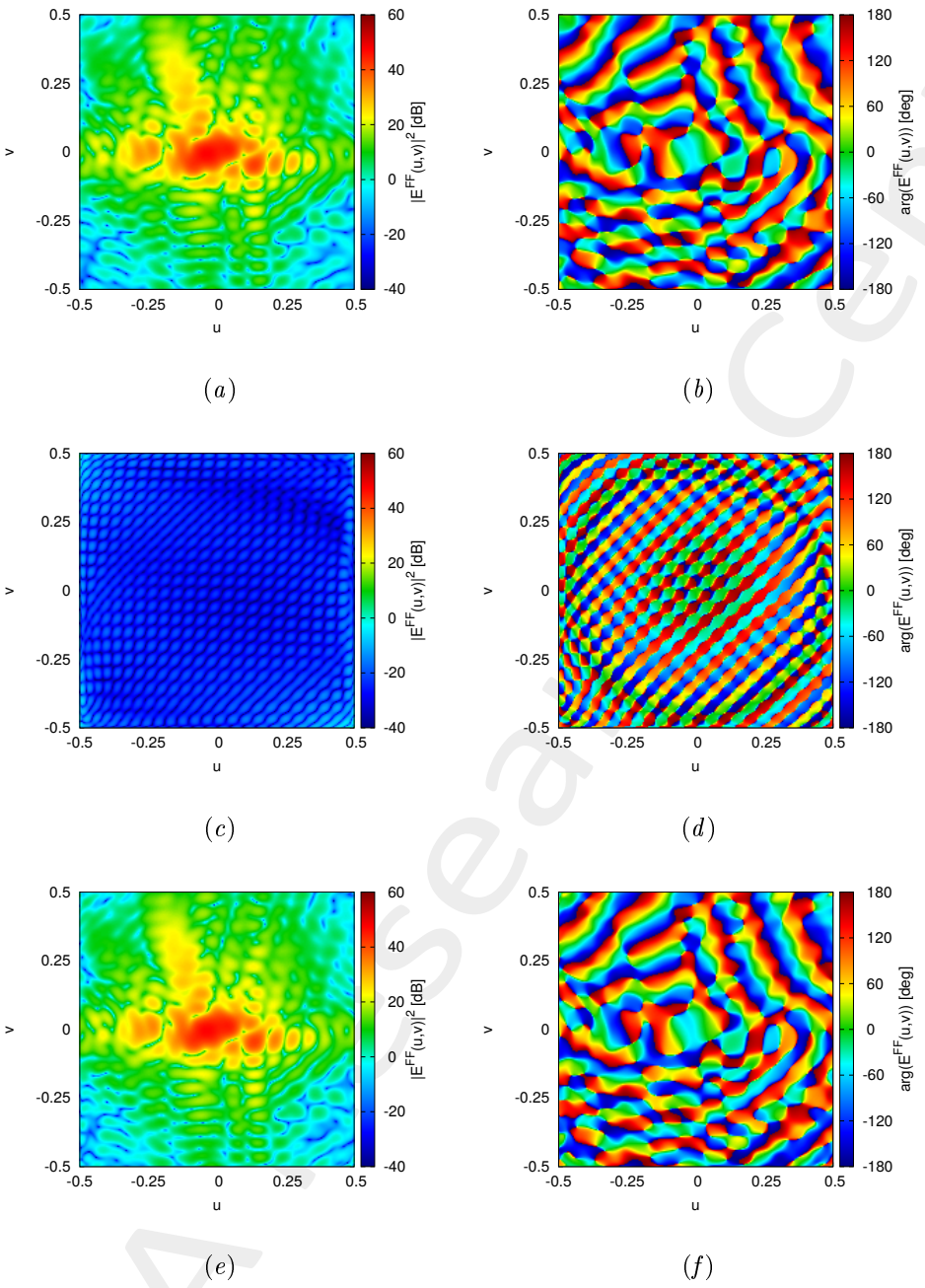

Figure 4: $(a)(c)(e)$ Magnitude and $(b)(d)(f)$ phase of the radiated field by $(a)(b)$, $J^{MN}(x,y)$, $(c)(d)$ $J^{NR}(x,y;\underline{\alpha})$, and $(e)(f)$ $J^{TOT}(x,y;\underline{\alpha})$.

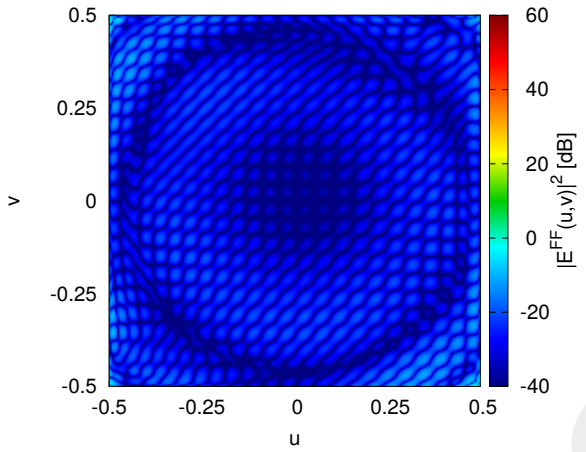

Figure 5: Magnitude of the difference between the radiated fields by $J^{MN}(x,y)$ and $J^{TOT}(x,y;\underline{\alpha})$.

1.2 Shape "triangle @ down left corner: 3 pixel side"

Parameters

- Number of reflectarray elements: $M = N = 55$;
- Operative frequency: $f = 14$ [GHz];
- Polarization: X-CO;
- Number of elements in the forbidden region: $Q = 6$;

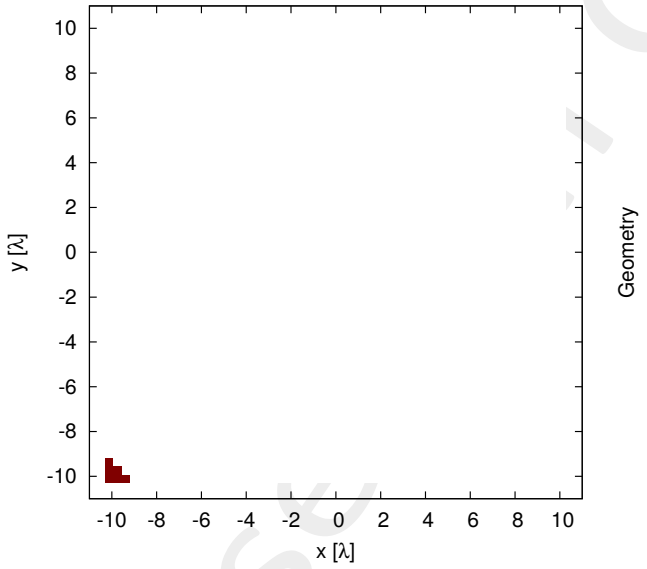

Figure 6: Geometry of forbidden region Ω.

Results

Magnitude and phase of the *NR* coefficients.

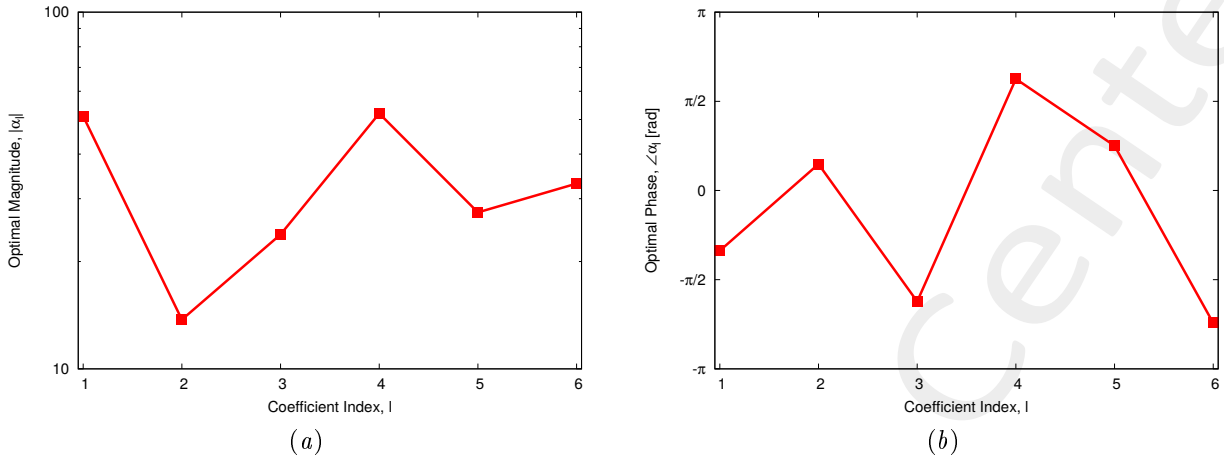

(a) (b)

Figure 7: Magnitude (a) and phase (b) of the solution.

Currents Distribution

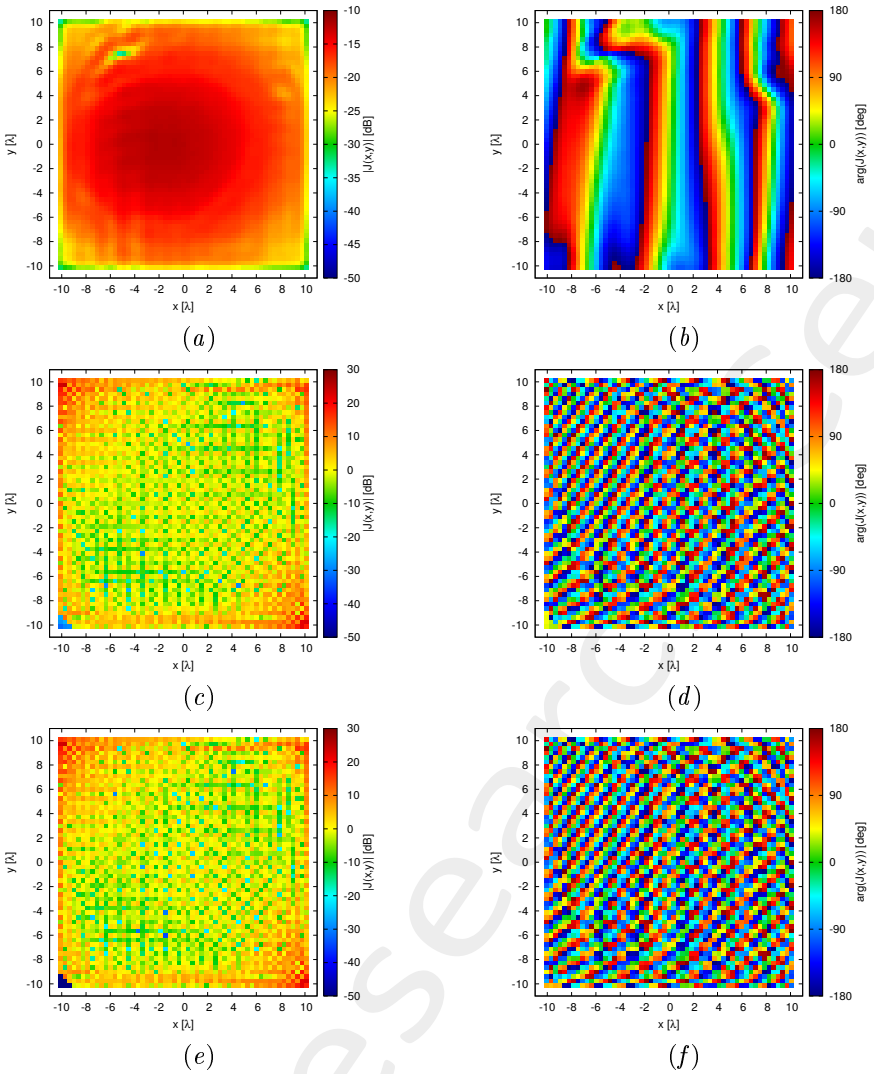

Figure 8: $(a)(c)(e)$ Magnitude and $(b)(d)(f)$ phase $(a)(b)$ of $J^{MN}(x,y)$, $(c)(d)$ $J^{NR}(x,y;\underline{\alpha})$, and $(e)(f)$ $J^{TOT}(x,y;\underline{\alpha})$.

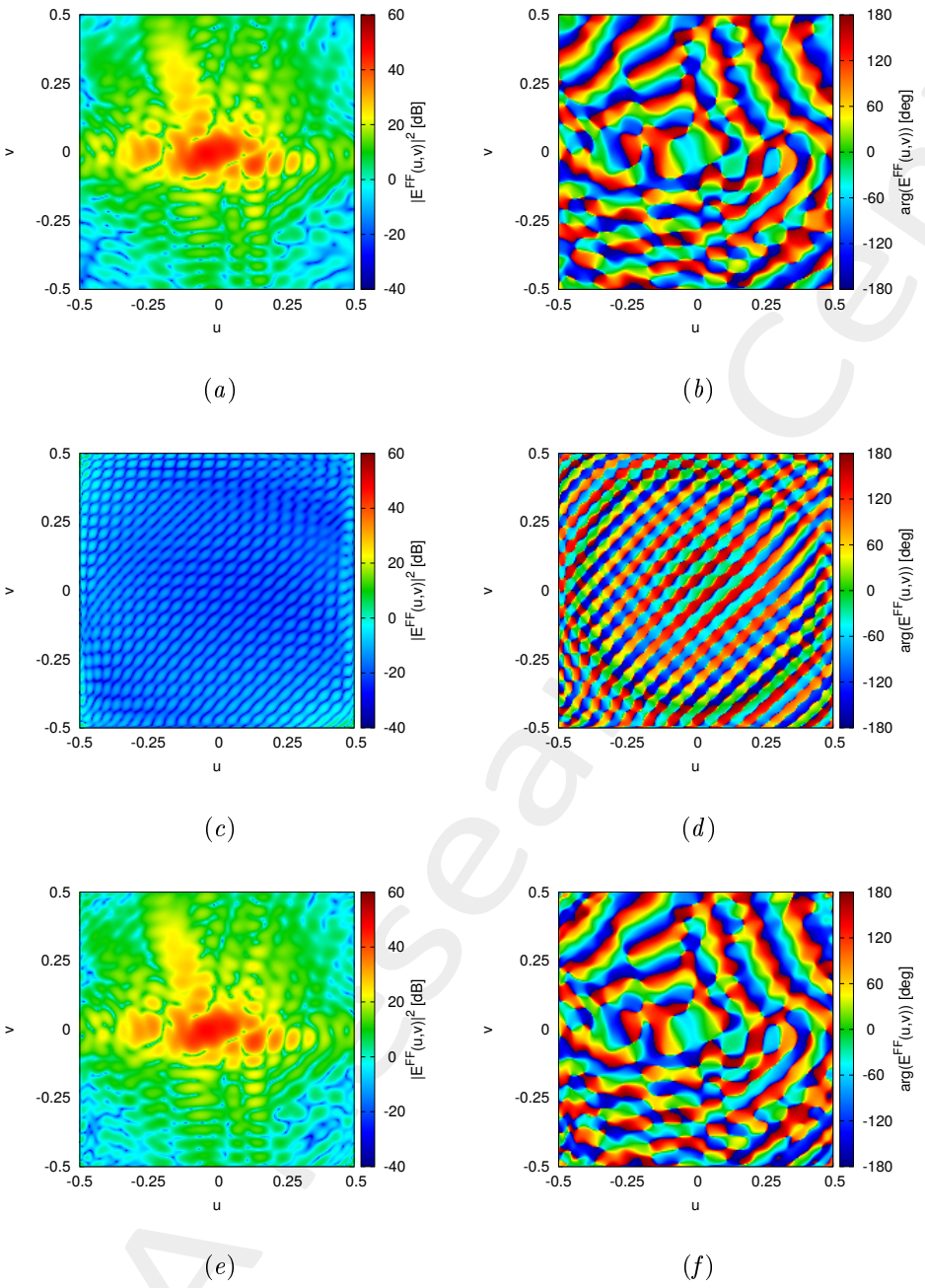

Figure 9: $(a)(c)(e)$ Magnitude and $(b)(d)(f)$ phase of the radiated field by $(a)(b)$, $J^{MN}(x,y)$, $(c)(d)$ $J^{NR}(x,y;\underline{\alpha})$, and $(e)(f)$ $J^{TOT}(x,y;\underline{\alpha})$.

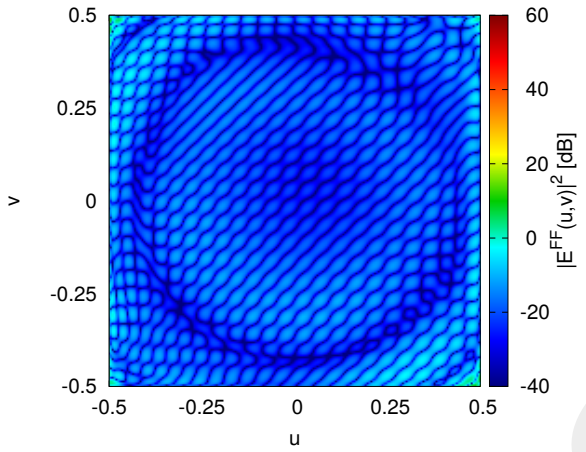

Figure 10: Magnitude of the difference between the radiated fields by $J^{MN}(x,y)$ and $J^{TOT}(x,y;\underline{\alpha})$.

1.3 Shape "triangle @ down left corner: 5 pixel side"

Parameters

- Number of reflectarray elements: $M = N = 55$;
- Operative frequency: $f = 14$ [GHz];
- Polarization: X-CO;
- Number of elements in the forbidden region: $Q = 15$;

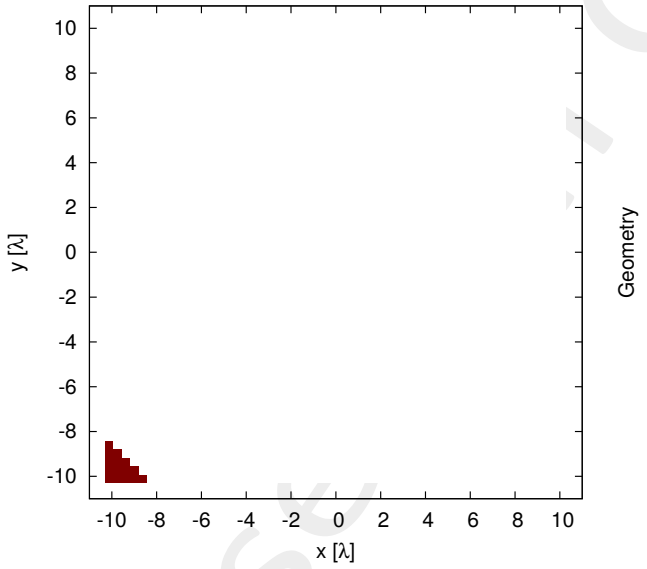

Figure 11: Geometry of forbidden region Ω.

Results

Magnitude and phase of the *NR* coefficients.

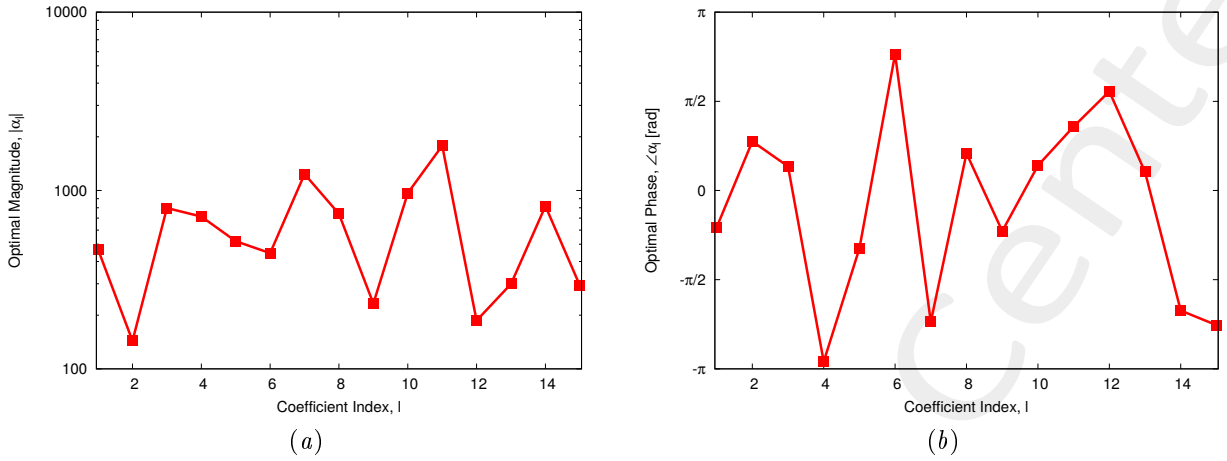

(*a*) (*b*)

Figure 12: Magnitude (*a*) and phase (*b*) of the solution.

Currents Distribution

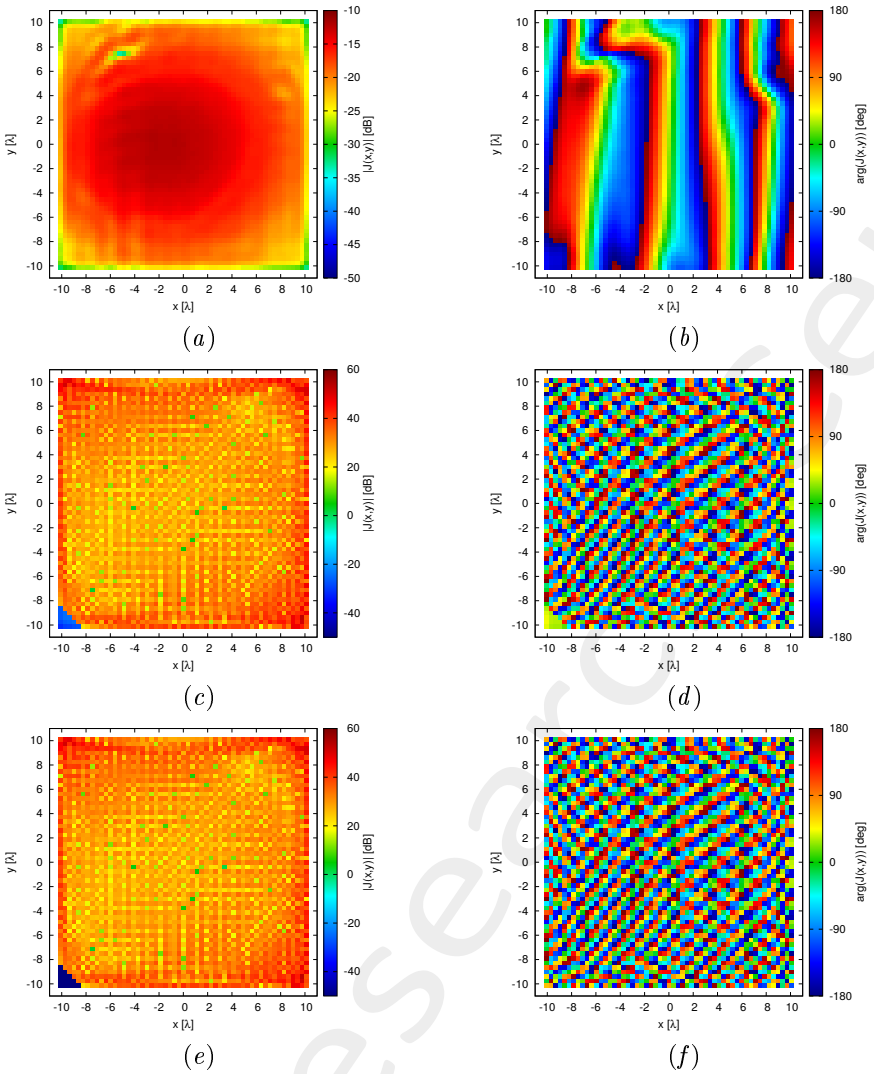

Figure 13: $(a)(c)(e)$ Magnitude and $(b)(d)(f)$ phase $(a)(b)$ of $J^{MN}(x,y)$, $(c)(d)$ $J^{NR}(x,y;\underline{\alpha})$, and $(e)(f)$ $J^{TOT}(x,y;\underline{\alpha})$.

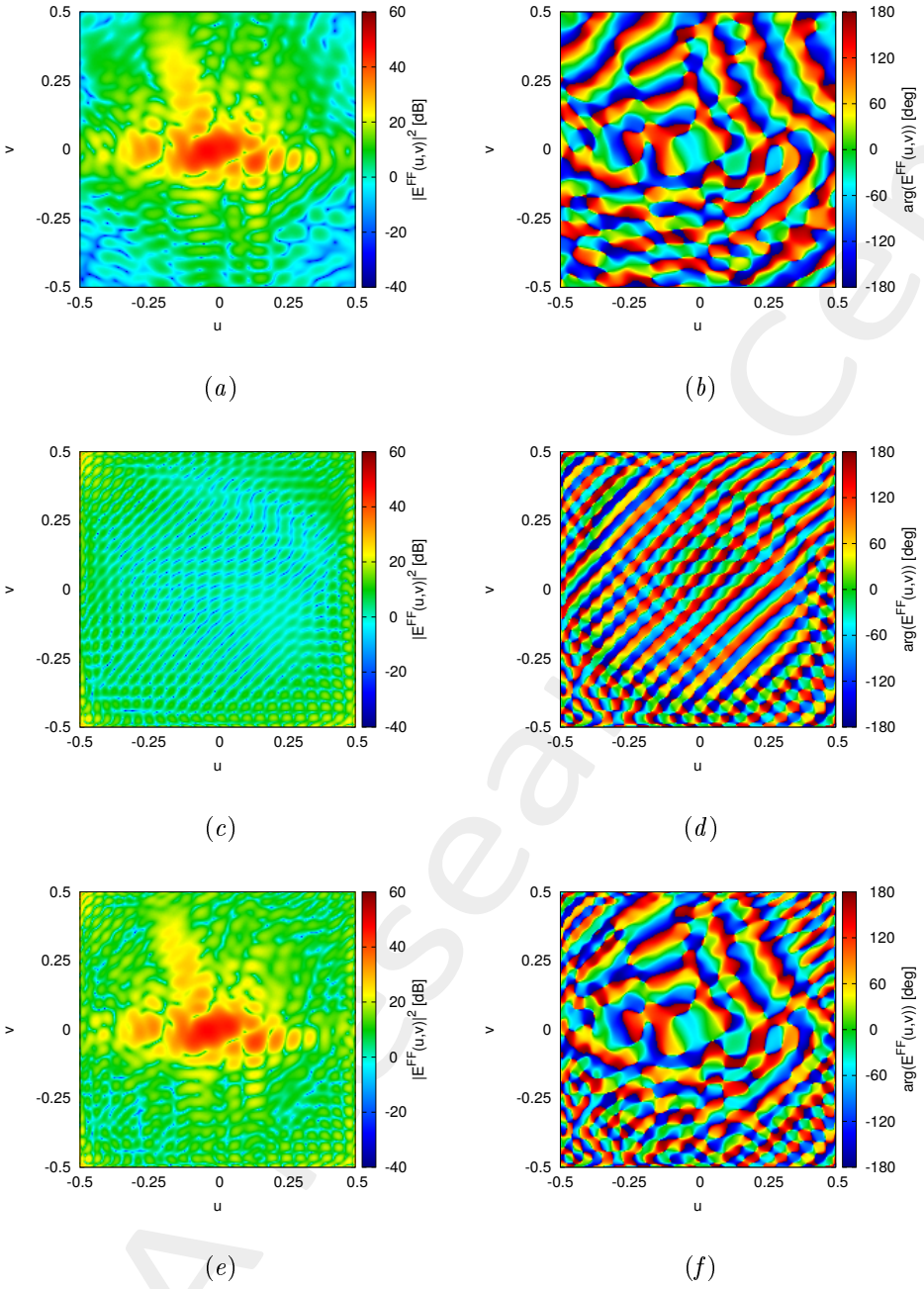

Figure 14: $(a)(c)(e)$ Magnitude and $(b)(d)(f)$ phase of the radiated field by $(a)(b)$, $J^{MN}(x,y)$, $(c)(d)$ $J^{NR}(x,y;\underline{\alpha})$, and $(e)(f)$ $J^{TOT}(x,y;\underline{\alpha})$.

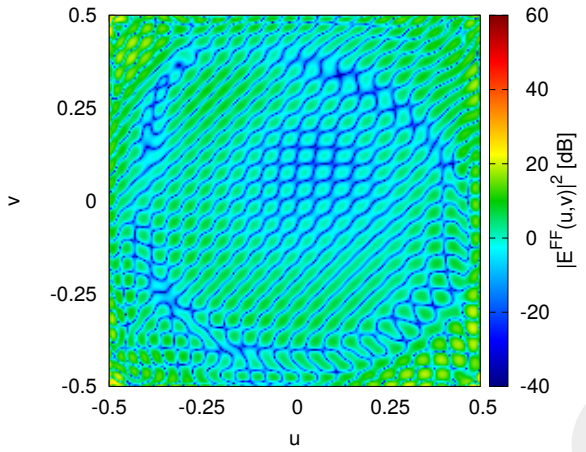

Figure 15: Magnitude of the difference between the radiated fields by $J^{MN}(x,y)$ and $J^{TOT}(x,y;\underline{\alpha})$.

1.4 Shape “triangle 10 pixel side @ down left 6-6”

Parameters

- Number of reflectarray elements: $M = N = 55$;
- Operative frequency: $f = 14$ [GHz];
- Polarization: X-CO;
- Number of elements in the forbidden region: $Q = 55$;

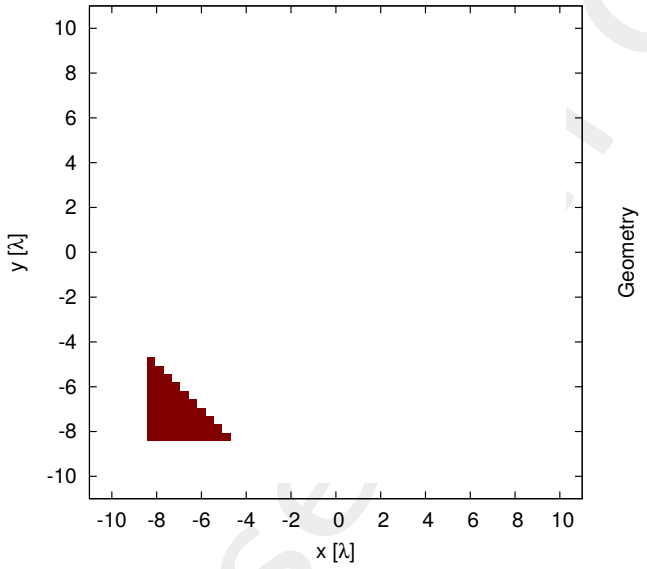

Figure 16: Geometry of forbidden region Ω.

Results

Magnitude and phase of the *NR* coefficients.

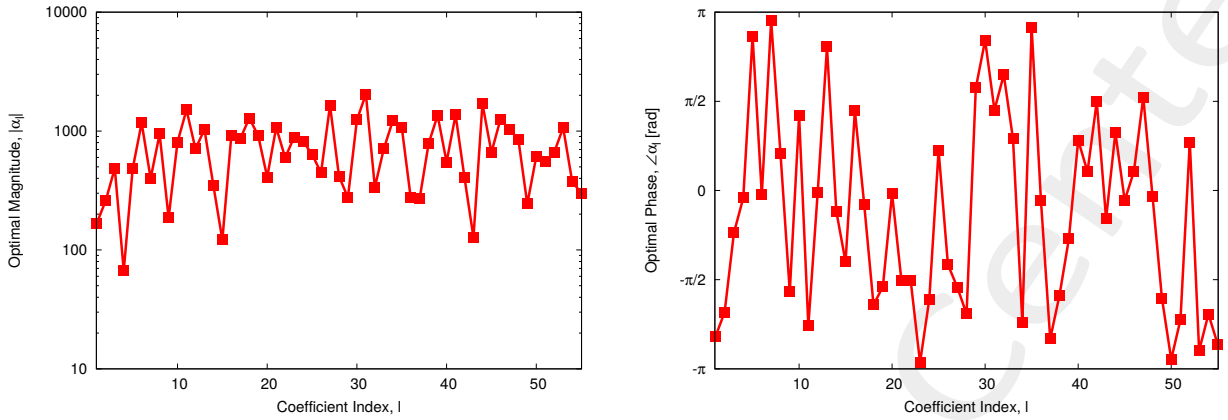

(*a*) (*b*)

Figure 17: Magnitude (*a*) and phase (*b*) of the solution.

Currents Distribution

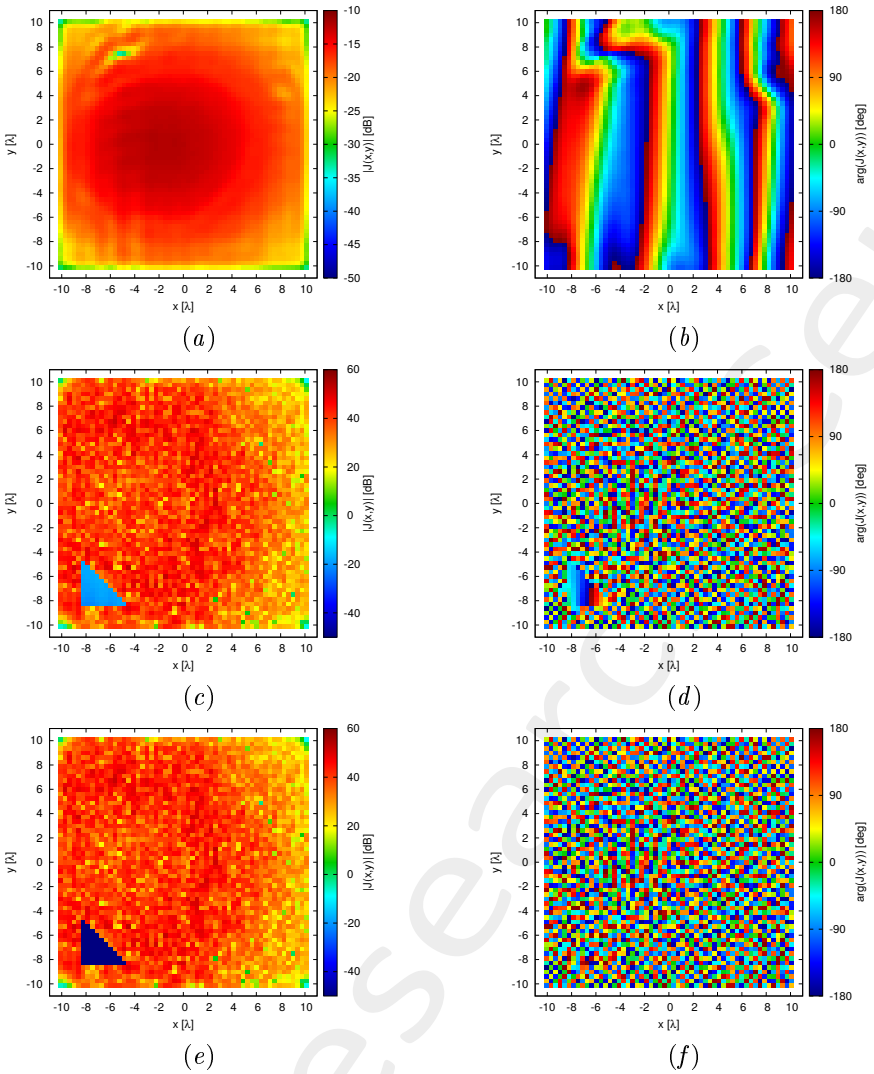

Figure 18: $(a)(c)(e)$ Magnitude and $(b)(d)(f)$ phase $(a)(b)$ of $J^{MN}(x,y)$, $(c)(d)$ $J^{NR}(x,y;\underline{\alpha})$, and $(e)(f)$ $J^{TOT}(x,y;\underline{\alpha})$.

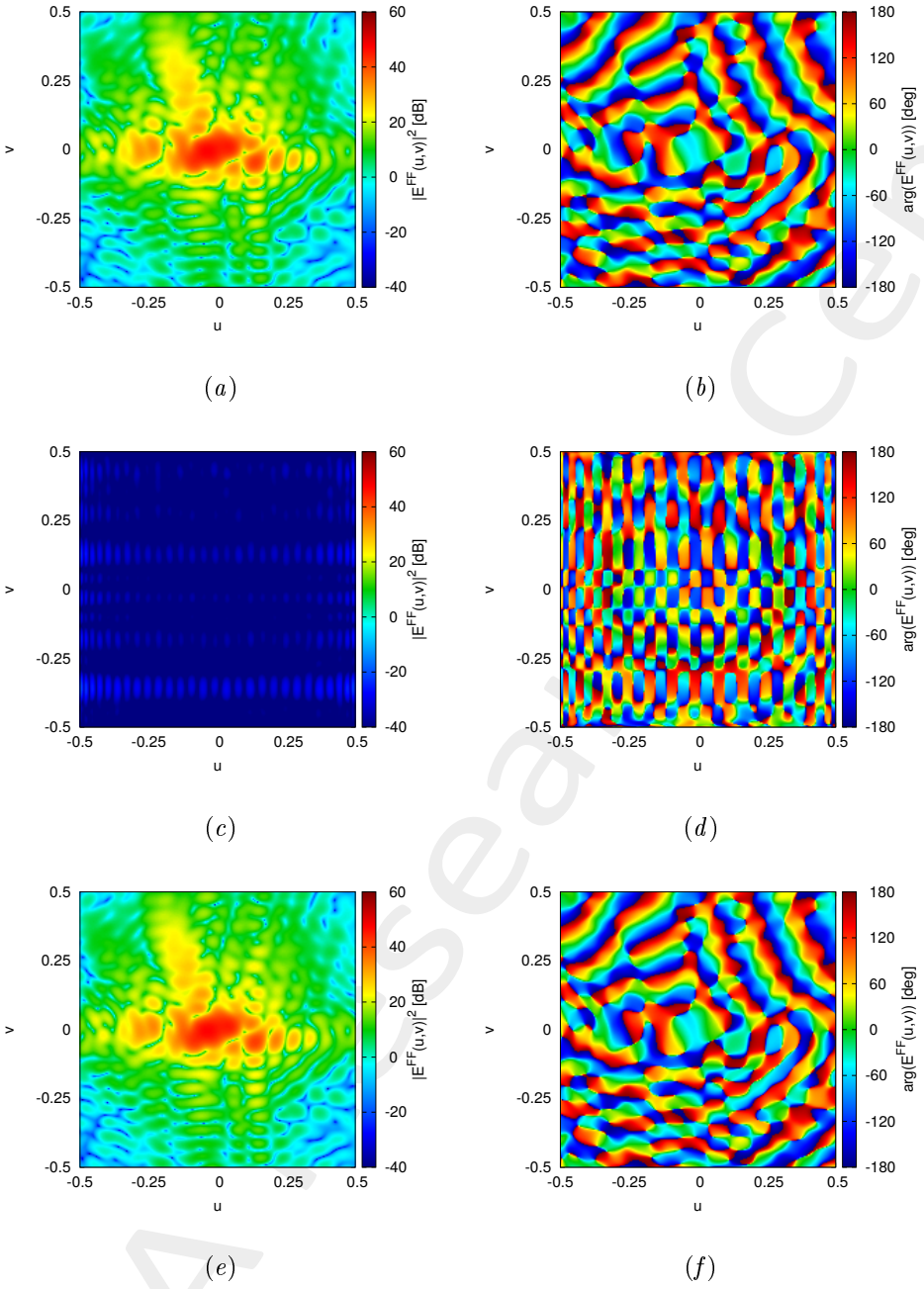

Figure 19: $(a)(c)(e)$ Magnitude and $(b)(d)(f)$ phase of the radiated field by $(a)(b)$, $J^{MN}(x,y)$, $(c)(d)$ $J^{NR}(x,y;\underline{\alpha})$, and $(e)(f)$ $J^{TOT}(x,y;\underline{\alpha})$.

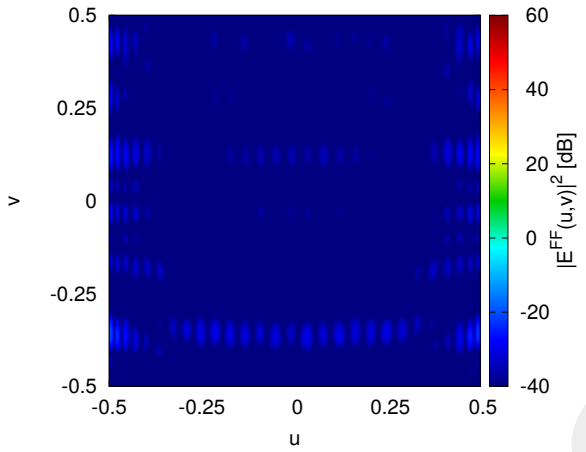

Figure 20: Magnitude of the difference between the radiated fields by $J^{MN}(x,y)$ and $J^{TOT}(x,y;\underline{\alpha})$.

1.5 Shape “triangle 10 pixel side @ down left 8-8”

Parameters

- Number of reflectarray elements: $M = N = 55$;
- Operative frequency: $f = 14$ [GHz];
- Polarization: X-CO;
- Number of elements in the forbidden region: $Q = 55$;
- $O = 55$.

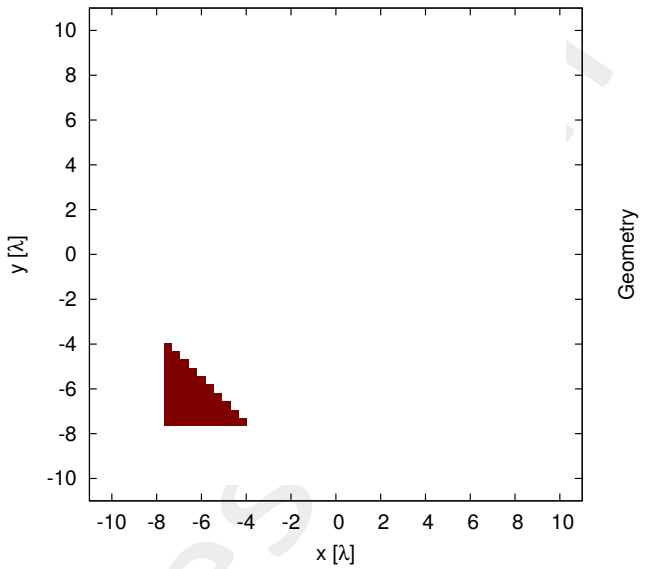

Figure 21: Geometry of forbidden region Ω.

Results

Magnitude and phase of the *NR* coefficients.

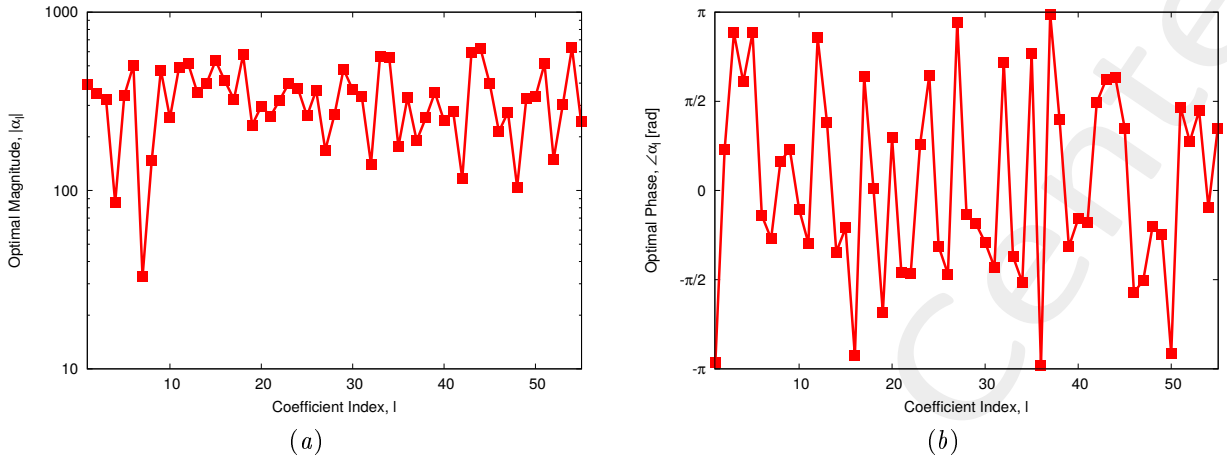

(a) (b)

Figure 22: Magnitude (a) and phase (b) of the solution.

Currents Distribution

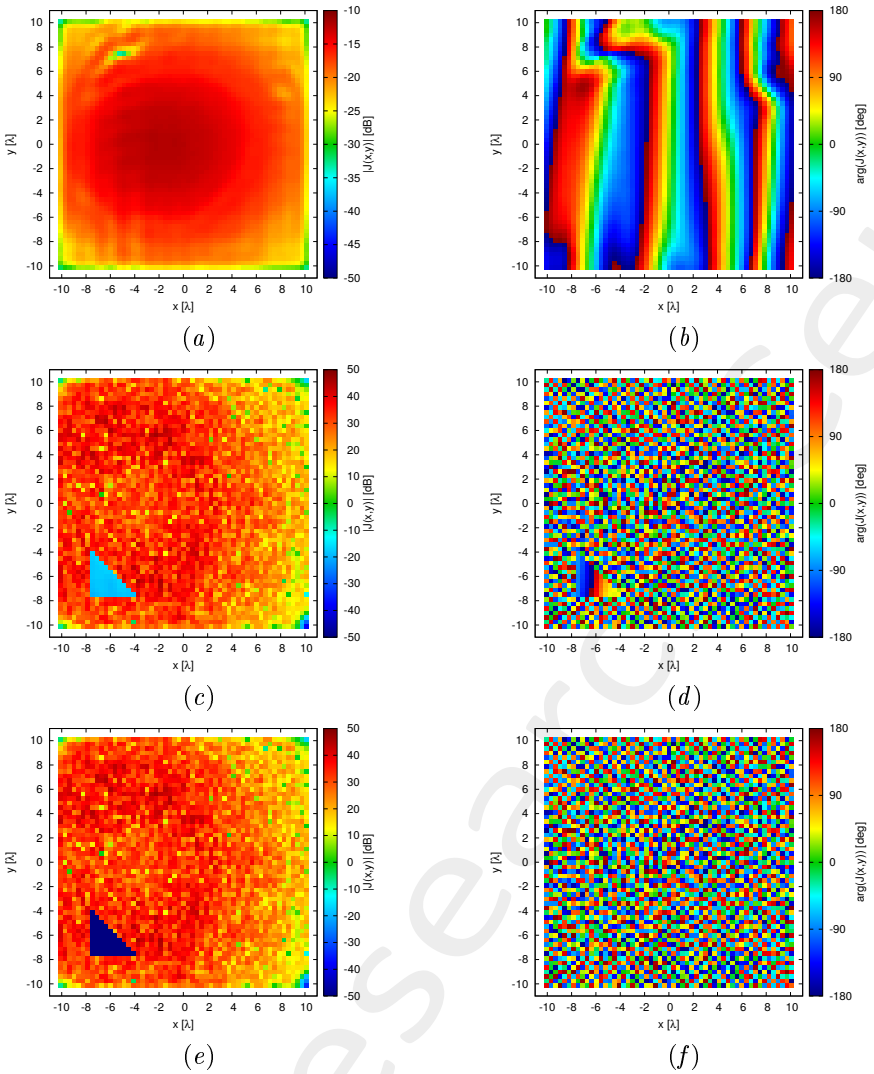

Figure 23: $(a)(c)(e)$ Magnitude and $(b)(d)(f)$ phase $(a)(b)$ of $J^{MN}(x,y)$, $(c)(d)$ $J^{NR}(x,y;\underline{\alpha})$, and $(e)(f)$ $J^{TOT}(x,y;\underline{\alpha})$.

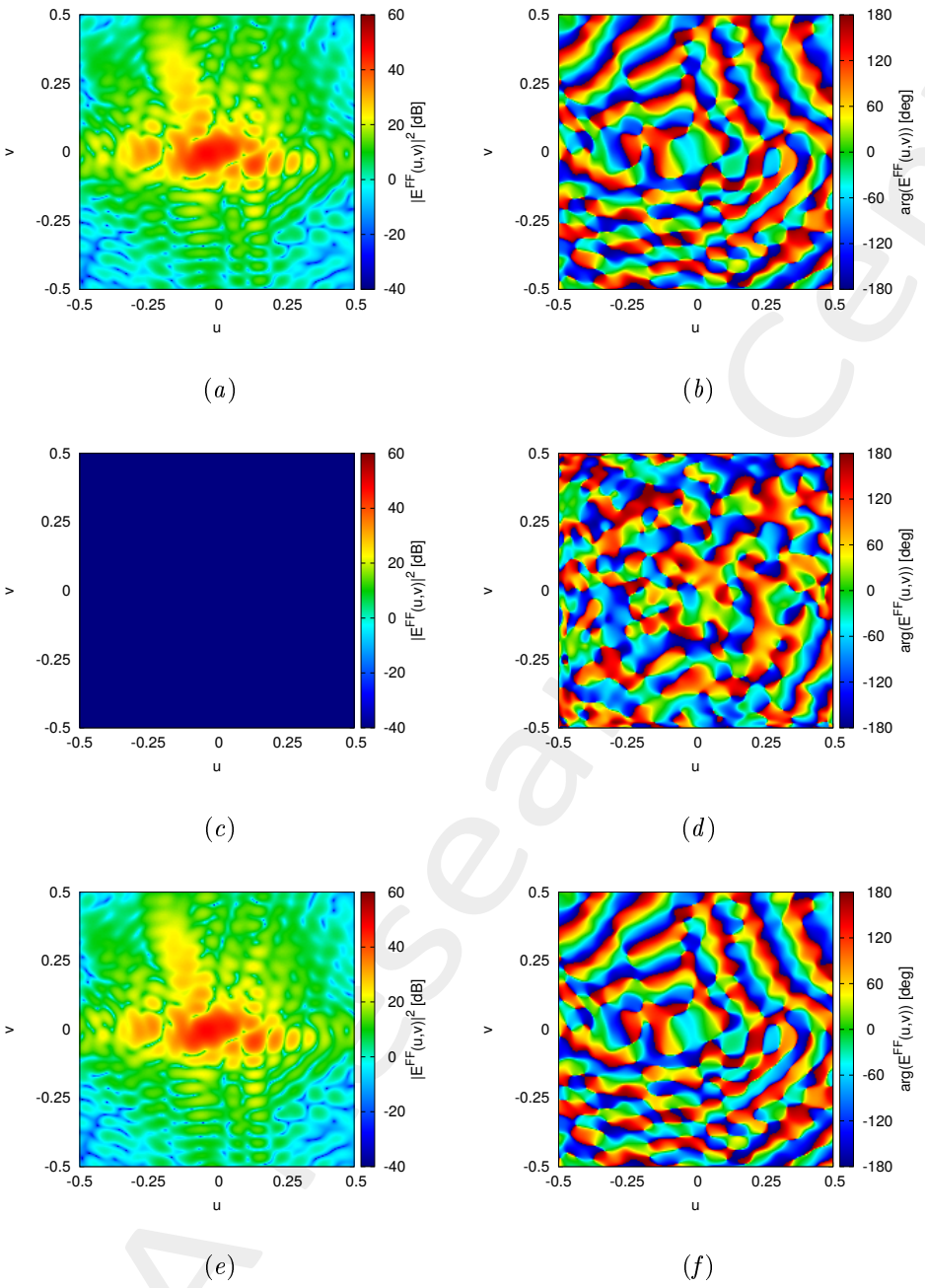

Figure 24: $(a)(c)(e)$ Magnitude and $(b)(d)(f)$ phase of the radiated field by $(a)(b)$, $J^{MN}(x,y)$, $(c)(d)$ $J^{NR}(x,y;\underline{\alpha})$, and $(e)(f)$ $J^{TOT}(x,y;\underline{\alpha})$.

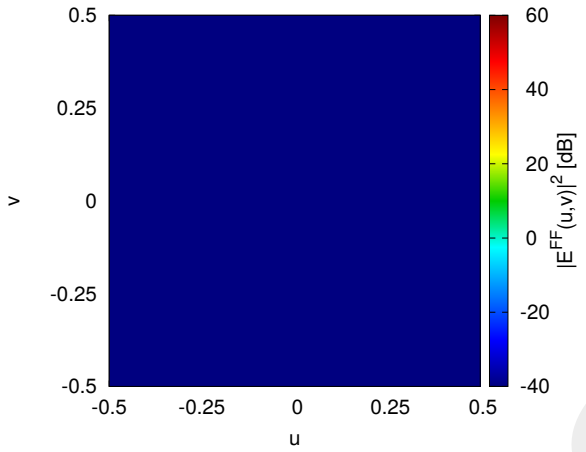

Figure 25: Magnitude of the difference between the radiated fields by $J^{MN}(x,y)$ and $J^{TOT}(x,y;\underline{\alpha})$.

References

[1] P. Rocca, G. Oliveri, R. J. Mailloux, and A. Massa, "Unconventional phased array architectures and design methodologies: A review," *Proc. IEEE*, vol. 104, no. 3, pp. 544-560, Mar. 2016.

[2] P. Rocca, L. Poli, N. Anselmi, M. Salucci, and A. Massa, "Predicting antenna pattern degradations in microstrip reflectarrays through interval arithmetic," *IET Microw., Antennas Propag.*, vol. 10, no. 8, pp. 817-826, Mar. 2016.

[3] M. Salucci, L. Tenuti, G. Oliveri, and A. Massa, "Efficient prediction of the EM response of reflectarray antenna elements by an advanced statistical learning method," *IEEE Trans. Antennas Propag.*, vol. 66, no. 8, pp. 3995-4007, Aug. 2018.

[4] M. Salucci, A. Gelmini, G. Oliveri, N. Anselmi, and A. Massa, "Synthesis of shaped beam reflectarrays with constrained geometry by exploiting non-radiating surface currents," *IEEE Trans. Antennas Propag.*, vol. 66, no. 11, pp. 5805-5817, Nov. 2018

[5] G. Oliveri, Y. Zhong, X. Chen, and A. Massa, "Multi-resolution subspace-based optimization method for inverse scattering," *J. Opt. Soc. Amer. A*, Opt. Image Sci., vol. 28, no. 10, pp. 2057-2069, Oct. 2011.

[6] L. Poli, G. Oliveri, F. Viani, and A. Massa, "MT-BCS-based microwave imaging approach through minimum-norm current expansion," *IEEE Trans. Antennas Propag.*, vol. 61, no. 9, pp. 4722-4732, Sep. 2013.

[7] N. Anselmi, P. Rocca, M. Salucci, and A. Massa, "Irregular phased array tiling by means of analytic schemata-driven optimization," *IEEE Trans. Antennas Propag.*, vol. 65, no. 9, pp. 4495-4510, Sep. 2017.

[8] L. Poli, P. Rocca, M. Salucci, and A. Massa, "Reconfigurable thinning for the adaptive control of linear arrays," *IEEE Trans. Antennas Propag.*, vol. 61, no. 10, pp. 5068-5077, Oct. 2013.

[9] L. Poli, G. Oliveri, P. Rocca, M. Salucci, and A. Massa, "Long-Distance WPT Unconventional Arrays Synthesis" *Journal of Electromagnetic Waves and Applications*, vol. 31, no. 14, pp. 1399-1420, Jul. 2017.

[10] M. Salucci, G. Gottardi, N. Anselmi, and G. Oliveri, "Planar thinned array design by hybrid analytical-stochastic optimization," *IET Microwaves, Antennas & Propagation*, vol. 11, no. 13, pp. 1841-1845, Oct. 2017.

[11] P. Rocca, T. Moriyama, N. Anselmi, and A. Massa, "Robust prediction of the radiated pattern features with uncertainties in reflectarray design," 2014 IEEE Antenna Conference on Antenna Measurements and Applications (IEEE CAMA 2014), Antibes Juan-les-Pins, France, pp. 1-3, November 16-19, 2014.

[12] G. Oliveri, A. Gelmini, M. Salucci, D. Bresciani, and A. Massa, "Exploiting non-radiating currents in reflectarray antenna design," 11th European Conference on Antennas and Propagation (EUCAP 2017), Paris, France, pp. 88-91, March 19-24, 2017.